Mater. Res. Soc. Symp. Proc. Vol. 962 © 2007 Materials Research Society 0962-P13-03

Electron Holography of Ferromagnetic Nanoparticles Encapsulated in Three-Dimensional Arrays of Aligned Carbon Nanotubes

Krzysztof K. Koziol[1], Takeshi Kasama[1,2], Rafal E. Dunin-Borkowski[1], Prabeer Barpanda[1], and Alan H. Windle[1]

[1]Department of Materials Science and Metallurgy, University of Cambridge, Pembroke Street, Cambridge, CB2 3QZ, United Kingdom

[2]The Institute of Physical and Chemical Research, Frontier Research System, Hatoyama, Saitama, 350-0395, Japan

ABSTRACT

Closely-spaced ferromagnetic nanoparticles are of interest for applications that include data storage, magnetic imaging and drug delivery. Here, we use off-axis electron holography and micromagnetic simulations to study the magnetic properties of iron nanoparticles encapsulated in three-dimensional arrays of carbon nanotubes. The nanotubes constrain the shapes, sizes and separations of the nanoparticles, as well protecting them from oxidation. We record magnetic induction maps from individual particles that each contain a single magnetic domain. We also discuss the use of electron holography to assess magnetostatic interactions between adjacent particles.

INTRODUCTION

Since their discovery [1, 2], carbon nanotubes have attracted considerable interest as a result of their outstanding mechanical, electronic and thermal properties. Here, we use off-axis electron holography [3, 4] in the transmission electron microscope (TEM) to characterise the magnetic properties of carbon nanotubes that have been synthesised in highly-aligned arrays using chemical vapour deposition (CVD) and contain closely-spaced ferromagnetic iron catalyst particles. We compare our measurements with magnetic induction maps determined from micromagnetic simulations. Our results provide high spatial resolution quantitative magnetic information that cannot be obtained using techniques such as magnetic force microscopy (MFM) [5] and magnetometry. The latter techniques have previously been applied to the characterization of the magnetic properties of carbon-related materials [6] and metallic particles formed within [7, 8] and on the surfaces of [9, 10] carbon nanotubes.

EXPERIMENTAL DETAILS

Carbon nanotubes were synthesised by CVD on quartz substrates from a toluene/ferrocene feedstock solution that decomposes into hydrocarbon species and metal particles. Highly-aligned nanotubes grow from the particles perpendicular to the substrate (Fig. 1), with excess iron encapsulated in the nanotubes. The encapsulated particles are typically spaced few hundred nanometres apart and approximately ellipsoidal in shape. Both the diameter

of the nanotubes and the spacing of the particles can be controlled by tuning the CVD process [11].

Off-axis electron holograms of individual carbon nanotubes were acquired at 300 kV using a Philips CM300 field emission gun TEM. The technique involves using an electron biprism to overlap an electron wave that has passed through the region of interest on the specimen with a reference wave that has passed only through vacuum. The resulting holographic interference fringes can be used to obtain the amplitude and phase shift of the electron wave that has passed through the specimen. Unwanted contributions to the recorded phase shift, arising from variations in the mean inner potential of the specimen, were removed by using the conventional TEM objective lens to saturate the nanoparticles magnetically parallel and antiparallel to their long axes. The magnetic contribution to the phase shift was then obtained by determining half the difference between phase images that had been acquired with the nanoparticles magnetized in opposite directions, with the microscope objective lens turned off and the sample at remanence. Contours were added to the magnetic contributions to the recorded phase images to reveal the magnetic flux density in the specimen quantitatively and non-invasively with nanometer spatial resolution [12].

Micromagnetic simulations based on solutions to the Landau-Lifshitz-Gilbert equation in the continuum micromagnetic limit [13] were used to obtain simulated phase images of isolated and closely-spaced ellipsoidal iron particles for comparison with the experimental observations. A maximum variation of 10^{-4} in the direction cosines of the local magnetic moments was used as the exit criterion for computing equilibrium states. A gyromagnetic frequency of 17.6 MHz/Oe and a damping constant of 1 were used, and the effects of thermal fluctuations were not included.

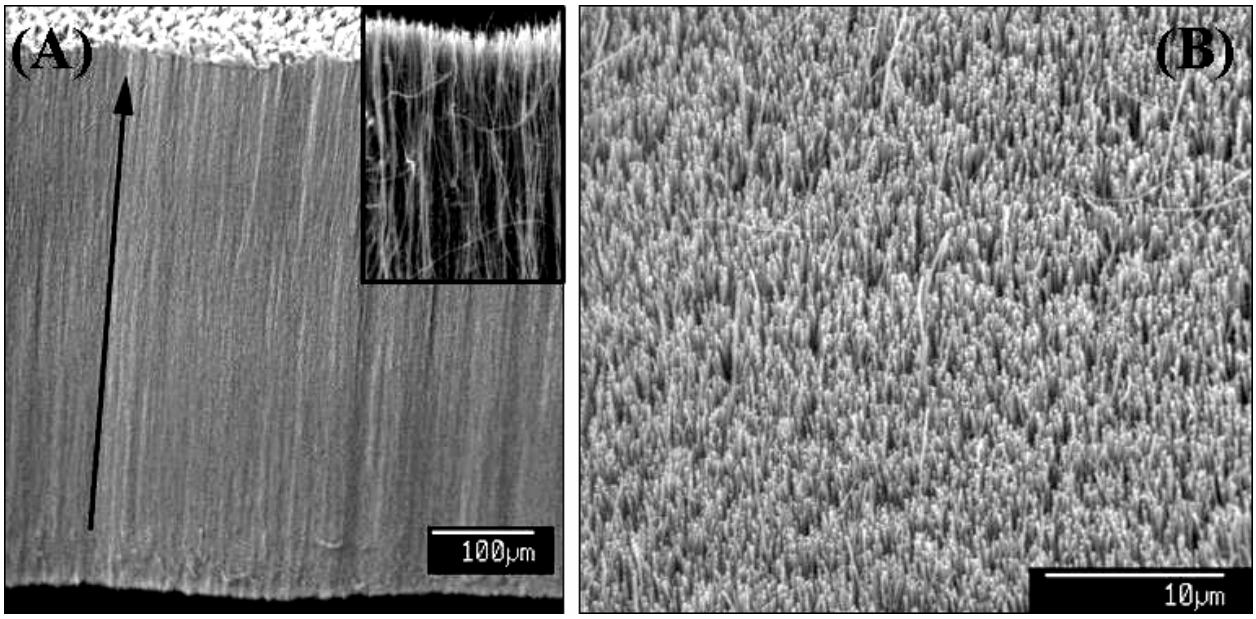

Figure1. Scanning electron micrographs showing (A) side and (B) top views of aligned carbon nanotube arrays that contain encapsulated ferromagnetic iron nanoparticles. The nanotube density of $5x10^6$ mm^{-2} is determined by the synthesis conditions used. The arrow in (A) indicates the direction of nanotube alignment.

RESULTS AND DISCUSSION

Figure 2 shows representative experimental results obtained from a 180-nm-diameter carbon nanotube that contains two iron particles, which have dimensions of 36 × 300 and 11 × 200 nm and are separated by a distance of 500 nm. The spacing of the magnetic phase contours shown in Fig. 2B, which were obtained using electron holography, is inversely proportional to the in-plane component of the magnetic induction in the specimen projected in the electron beam direction. The contours inside in each particle are not shown, for clarity. Figure 2B provides direct confirmation that both iron particles contain single magnetic domains. The larger particle displays a particularly clear and characteristic return flux. The micromagnetic simulation shown in Fig. 2C, which was performed using the measured sizes and separation of the particles and the nominal magnetic properties of pure iron, confirms the equilibrium domain state of both particles. The fit to the contours recorded from the smaller particle is poorer, most likely either because its diameter has been overestimated or because it may contain a large proportion of carbon than the larger particle, thereby altering its magnetic properties.

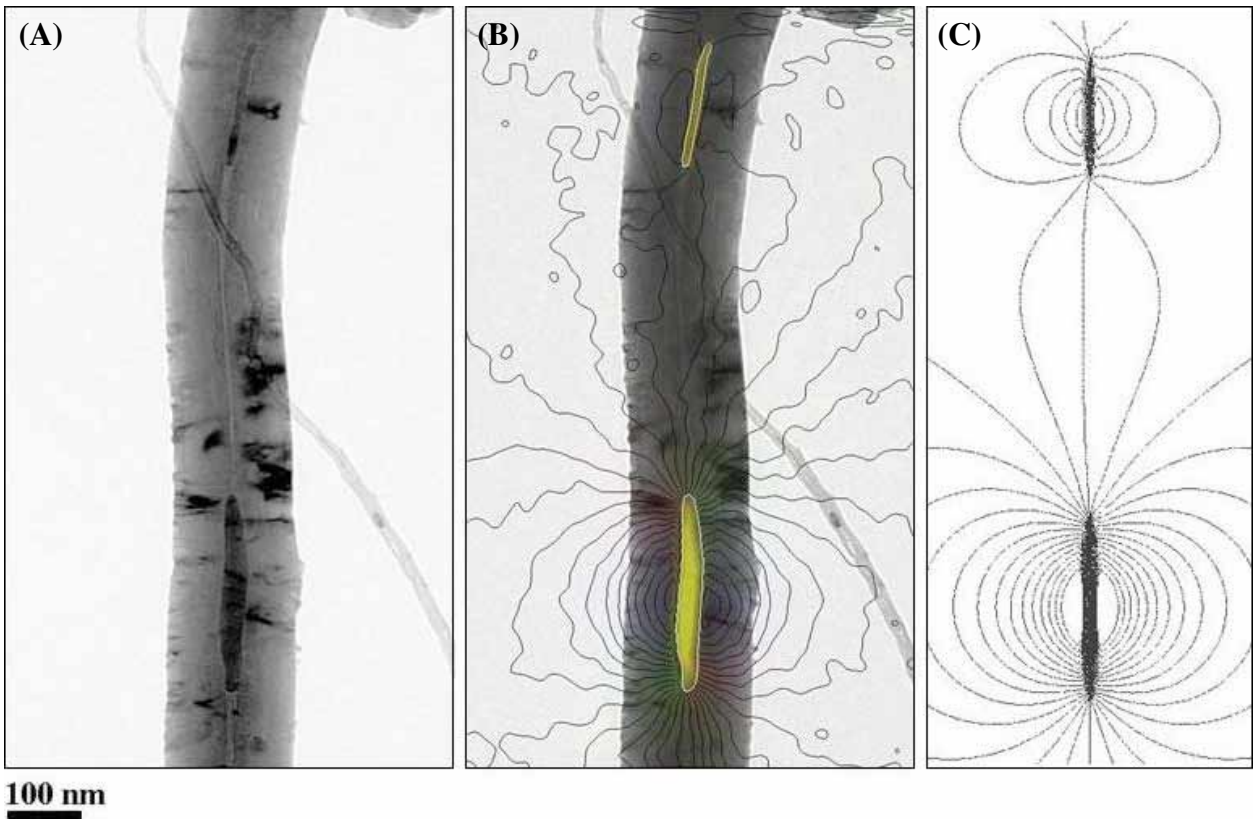

Figure 2. (A) Bright-field TEM image of a multi-walled carbon nanotube, approximately 180nm in diameter, containing 36-nm-diameter and 11-nm-diameter encapsulated iron crystals. (B) Magnetic phase contours, recorded using off-axis electron holography after magnetising the sample parallel and antiparallel to the direction of the nanotube axis, overlaid onto image (A). (C) Simulated magnetic induction map of two ellipsoidal iron particles with the dimensions and separation of the crystals shown in (A) and (B). The phase contour spacing in (B) and (C) is 0.098 radians.

The quantitative interpretation of the contours shown in Fig. 2 is complicated by the fact that their spacing is proportional to the magnetic induction projected in the electron beam direction [14]. Nevertheless, useful semi-quantitative information about magnetostatic interactions can be obtained by measuring their spacing, or equivalently the gradient of the magnetic contribution to the phase. This point is illustrated in Fig. 3, which shows simulations of ellipsoidal 36 × 300 nm Fe nanoparticles that are separated from each other by either 100 or 300 nm in one of two perpendicular directions. The spacing of the contours between the particles can be seen to depend on their separation, providing an indication of the strength of the projected magnetic induction between them.

Figure 4 shows the gradient of the magnetic phase shift at the mid-point of the collinear particles shown in the lower part of Fig. 3, determined from the micromagnetic simulations. The graph provides a measure of the influence of particle separation on the strength of the projected magnetic induction between the particles. As the phase gradient is also sensitive to the compositions and sizes of such particles, it could be used to provide an indication of the presence of non-ferromagnetic impurities such as carbon or silicon within them.

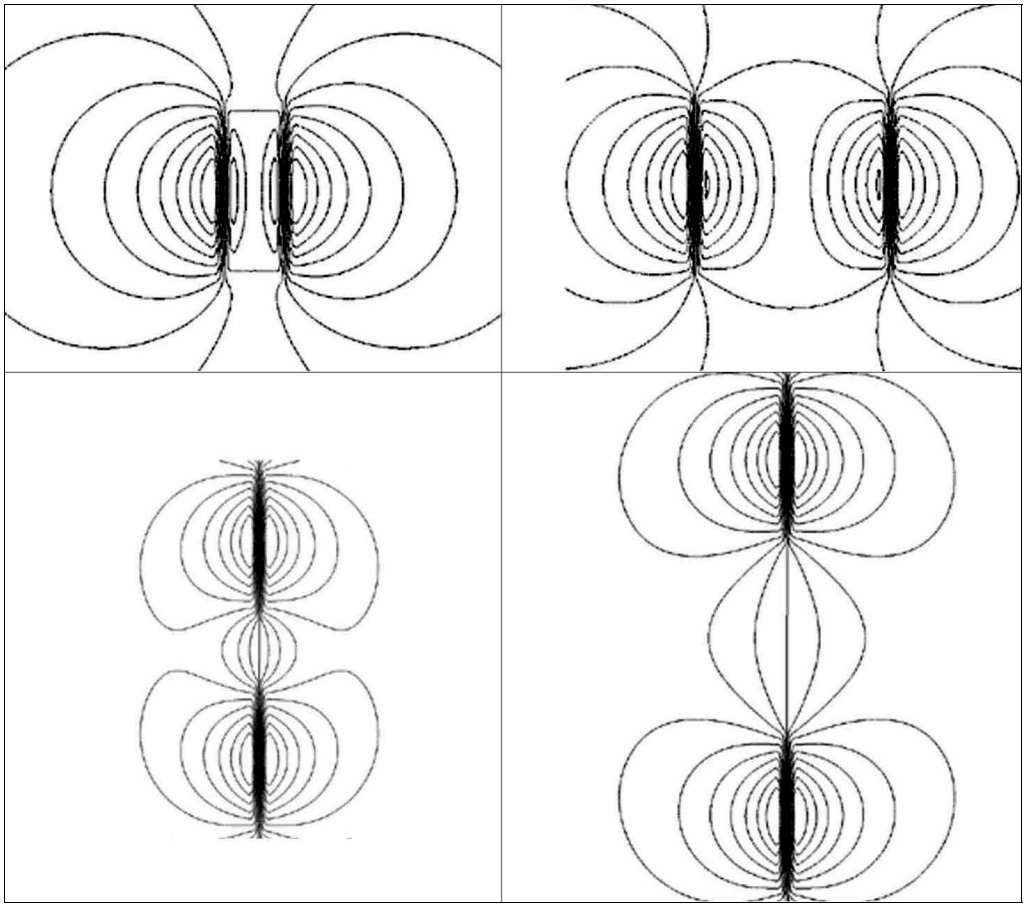

Figure 3. Micromagnetic simulations of magnetic phase contours generated for two ellipsoidal 36 × 300 nm ferromagnetic Fe nanoparticles separated from each other either laterally (top) or collinearly (bottom) by a distance of 100 nm (left) or 300 nm (right).

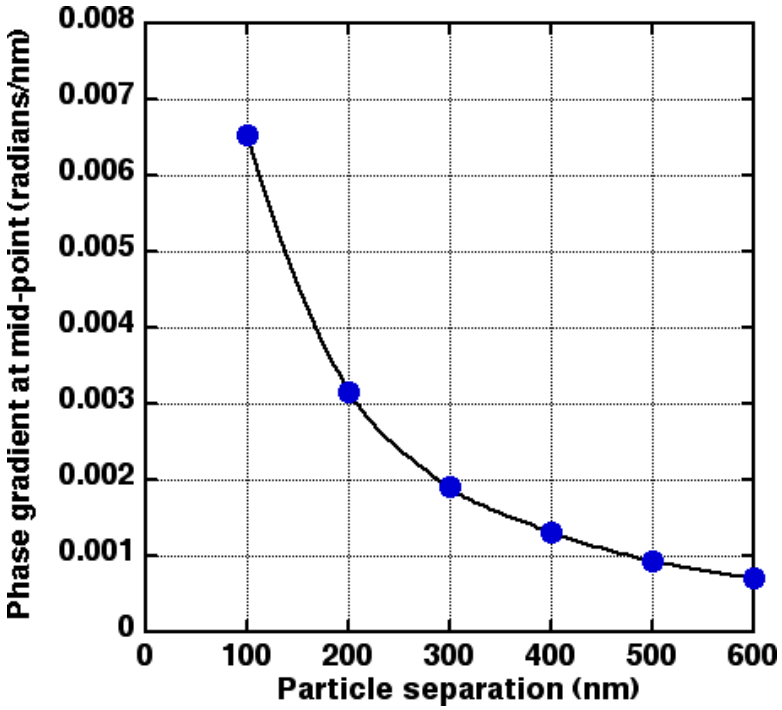

Figure 4. Phase gradient measured from micromagnetic simulations such as those shown in the lower part of Fig. 3, measured mid-way between two collinear ellipsoidal 36 × 300 nm ferromagnetic Fe nanoparticles as a function of their separation.

CONCLUSIONS

Off-axis electron holography has been used to record magnetic induction maps from individual ellipsoidal ferromagnetic iron nanoparticles encapsulated in multi-walled carbon nanotubes. The measurements show that the nanoparticles contain single magnetic domains. Results obtained from a 36 × 300 nm particle are consistent with magnetic phase contours determined from micromagnetic simulations that incorporate the magnetic properties of bulk iron. Simulations have been used to assess the influence of interparticle separation on phase contour spacing, and hence on magnetostatic interactions between adjacent nanoparticles.

Results similar to those obtained in the present study may be useful for understanding how the magnetic properties of such nano-composite materials may be tailored for use in applications such as information storage, magnetic imaging [15] and electromagnetic shielding.

ACKNOWLEDGMENTS

We are grateful to the Royal Society for financial support.

REFERENCES

1. A. Oberlin, M. Endo, and T. Koyama, *Journal of Crystal Growth* **32**, 335-349 (1976).
2. S. Iijima, *Nature* **354**, 56-58 (1991).
3. L. Marton, *Phys. Rev.* **85**, 1057-1058 (1952).
4. A. Orchowski, W. D. Rau, and H. Lichte, *Phys. Rev. Lett*. **74**, 399-402 (1995).
5. O. Cespedes, M. S. Ferreira, S. Sanvito, M. Kociak, and J. M. D. Coey, *J. Phys-condens. Mat.* **16**, L155-L161 (2004).
6. A. V. Rode, E. G. Gamaly, A. G. Christy, J. G. F. Gerald, S. T. Hyde, R. G. Elliman, B. Luther-Davies, A. I. Veinger, J. Androulakis, and J. Giapintzakis, *Phys. Rev. B* **70**, 054407 (2004).
7. J. W. Jang, *Phys. Stat. Sol. B* **241**, 1605–1608 (2004).
8. N. Keller, C. Pham-Huu, T. Shiga, C. Estournes, J. M. Greneche, and M. J. Ledoux, *Journal of Magnetism and Magnetic Materials* **272,** 1642–1644 (2004).
9. B. C. Satishkumar, Erasmus M. Vogl, A. Govindaraj, and C. N. R. Rao, *J. Phys. D: Appl. Phys.* **29**, 3173-3176 (1996).
10. X. Q. Yan, X. P. Gao, Y. Li, Z. Q. Liu, F. Wu, Y. T. Shen, and D. Y. Song, *Chem. Phys. Lett.* **372**, 336-341 (2003).
11. C. Singh, M. S. P. Shaffer, and A. H. Windle, *Carbon*, **41**, 359-368 (2003).
12. R. E. Dunin-Borkowski, T. Kasama, A. Wei, S. L. Tripp, M. J. Hytch, E. Snoeck, R. J. Harrison, and A. Putnis, *Microsc. Res. Techn.* **64**, 390 (2004).
13. http://llgmicro.home.mindspring.com/
14. T. Fujita, M. Chen, X. Wang, B. Xu, K. Inoke, and K. Yamamoto, *J. Appl. Phys.* **101**, 014323 (2007).
15. T. Arie, H. Nishijima, S. Akita, Y. Nakayama, *J. Vac. Sci. Technol. B*, **18,** 104-106 (2000).